Journal of Hazardous Materials 205–206 (2012) 179–188

Contents lists available at SciVerse ScienceDirect

Journal of Hazardous Materials

journal homepage: www.elsevier.com/locate/jhazmat

Preparation of molecularly imprinted nanoparticles with superparamagnetic susceptibility through atom transfer radical emulsion polymerization for the selective recognition of tetracycline from aqueous medium

Jiangdong Dai [a], Jianming Pan [a], Longcheng Xu [a], Xiuxiu Li [a], Zhiping Zhou [c], Rongxian Zhang [a], Yongsheng Yan [a,b,*]

[a] School of Chemistry and Chemical Engineering, Jiangsu University, Zhenjiang 212013, China
[b] State Key Laboratory of Natural and Biomimetic Drugs, Peking University, Beijing, 100191, China
[c] School of Material Science and Engineering, Jiangsu University, Zhenjiang 212013, China

ARTICLE INFO

Article history:
Received 18 November 2011
Received in revised form
19 December 2011
Accepted 20 December 2011
Available online 29 December 2011

Keywords:
Magnetic molecularly imprinted nanoparticles
Atom transfer radical emulsion polymerization
Selective recognition
Aqueous medium
Tetracycline

ABSTRACT

In the work, we reported an effective method for the preparation of molecularly imprinted nanoparticles with superparamagnetic susceptibility through atom transfer radical emulsion polymerization (ATREP), and then as-prepared magnetic molecularly imprinted nanoparticles (MMINs) were evaluated as adsorbents for selective recognition of tetracycline (TC) molecules from aqueous medium. The resulting nanoparticles were characterized by FT-IR, TGA, VSM, SEM and TEM. The results demonstrated MMINs with a narrow diameter distribution were cross-linked with modified Fe_3O_4 particles, composed of imprinted layer and exhibited good magnetic sensitivity, magnetic and thermal stability. Batch rebinding studies were carried out to determine the specific adsorption equilibrium, kinetics, and selective recognition. The estimated adsorption capacity of MMINs towards TC by the Langmuir isotherm model was 12.10 mg g^{-1} at 298 K, which was 6.33 times higher than that of magnetic non-molecularly imprinted nanoparticles (MNINs). The kinetic property of MMINs was well-described by the pseudo-second-order rate equation. The results of selective recognition experiments demonstrated outstanding affinity and selectivity towards TC over competitive antibiotics. The reusability of MMINs showed no obviously deterioration at least five repeated cycles in performance. In addition, the MMINs prepared were successfully applied to the extraction of TC from the spiked pork sample.

1. Introduction

Due to the good activity against acute diseases caused by gram-positive and gram-negative bacteria, tetracyclines (TCs), as valid veterinary medicine, are commonly used to cure several infectious diseases for prevention and treatment of farm animals or to promote growth as feed additives [1]. Following administration, TCs are poorly absorbed by the digestive system with mostly excreted unmetabolized, and a portion of them still remains biologically active in animal waste [2]. Then the persistent antibiotics existed in animal manure contribute to the toxic effect as well as the transfer and spread of antibiotic resistant genes among microorganisms [3]. In previous studies, a fact that exposure of TCs residue in soil [4] and water environment [5] could result in a significant ecological concern has been proved. Because of broad-spectrum antimicrobial activity and low cost, the wide applications of TCs have led to fairly concerns with regard to unsafe residue in animal-production foods such as milk, meat, egg, cheese, and honey [6–9], which could be directly toxic or else provoke allergic response in some hypersensitive individuals [10]. Therefore, it is of great necessity to development efficient and inexpensive treatment methods for the selective removal of such compounds from the environment.

Molecularly imprinted polymers (MIPs), possessing tailor-made recognition sites, exhibit the ability of specifically rebinding to a target molecule in preference to analogous compounds. In order to fabricate the specific binding sites, the co-polymerization of functional and cross-linking monomers around a template molecule in a suitable porogenic solution is firstly conducted, which results in creating a three-dimensional polymeric matrix. Then the template is removed from the polymeric matrix by chemical reaction or extraction, which leaves behind specific binding sites in MIPs complementary to the template in size, geometry, and chemical functionality [11]. Owing to the high specificity and selectivity, as well as favorable thermal, mechanical and chemical stability, MIPs have been widely used as artificial receptors in solid phase extraction [12], chromatography separation [13], chemical sensors

* Corresponding author. Tel.: +86 0511 88790683; fax: +86 0511 88791800.
E-mail address: djdxxx123@163.com (Y. Yan).

0304-3894/$ – see front matter © 2011 Elsevier B.V. All rights reserved.
doi:10.1016/j.jhazmat.2011.12.056

[14], catalysis [15], and many other applications. However, the full potential of MIPs will not be achieved until some of their inherent limitations are solved, such as low binding capacity, poor accessibility of the binding sites, and heterogeneous binding site distribution [16].

Traditional MIP bulks have to be crushed, ground and sieved to obtain the desired particles. The tedious process often produces particles that are irregular in size and shape, as well as low rebinding capacity and poor site accessibility to target [17]. Because of extremely high surface-to-volume ratio of imprinted nanomaterials, most of template molecules can situate at the surface or in the proximity of materials surface. Thus, all the imprinted templates can be completely removed from the highly cross-linked polymer matrix and the binding sites obtained are all valid for the target. Molecular imprinting nanotechniques have been considered to be an effective and promising solution to these drawbacks mentioned above by overcoming mass transfer limitations and improving the accessibility [18].

Nowadays, MIPs are commonly prepared by free radical polymerization (FRP), photopolymerization [19], and electropolymerization [20]. FRP is the mostly adopted technique because of its tolerance for mild experimental conditions and various applicable monomer and template molecule species. However, conventional free radical polymerizations (FRP) have little control over structures due to several inherent features of FRP, including slow initiation, fast chain propagation, and termination reactions. Then the heterogeneous structures within polymer networks are observed from the MIPs prepared by FRP, which would have great disadvantage on the binding sites, such as broad binding site heterogeneity and the relatively low affinity and selectivity [21]. In contrast, many works reported the polymer networks with homogeneous structures preparing via controlled radical polymerization (CRP) methods. Recently, atom transfer radical polymerization (ATRP), as a new class of CRP, has been utilized as a new imprinting technology to improve imprinting properties. ATRP has succeeded in preparation of surface-imprinted polymers [22–26], MIP nanotube membranes [27] and microspheres [28]. However, the majority of imprinting processes combined with ATRP were carried out in organic solvents, such as acetonitrile and dichloromethane, which are relatively expensive and toxic. The achievement of molecular imprinting and recognition in green solvent such as water is a challenging but tremendously significant task. To the best of our knowledge, ATRP has never been used in emulsion-system to prepare the MIPs. The MIPs prepared by atom transfer radical emulsion polymerization (ATREP) has the advantages of ATRP and emulsion polymerization, which can supply with both the homogeneous structures and nanoparticles, respectively.

When magnetically susceptible materials like Fe_3O_4 nanoparticles are incorporated into the imprinted polymers, magnetic MIPs will have magnetically susceptible characteristic and selectivity to the target. The magnetic MIPs captured targets can be easily collected by an external magnetic field without additional centrifugation or filtration, which makes separation easier, faster and more efficient. The combination of the superparamagnetic nanoparticles and MIPs will obviously significantly increase the scope of their potential applications.

Here, this paper was the first attempt to synthesize molecularly imprinted nanoparticles with superparamagnetic susceptibility by atom transfer radical emulsion polymerization (ATREP) and recognize TC from aqueous solution. The synthesized Fe_3O_4 nanoparticles were modified by γ-methacryloxypropyltrimethoxysilane (KH-570) to avoid the magnetite leakages. Then the obtained Fe_3O_4-KH570 was used as magnetically susceptible copolymer monomer. The prepolymerization of methacrylic acid (MAA) and TC was performed in the surfactant solution. Then, ethylene glycol dimethacrylate (EGDMA) as cross-linker, copolymer monomer, and initiator system were added into the solution, polymerization was carried out. The characterization, magnetite leakage, adsorption capacity, kinetics, and selectivity of the MMINs were investigated in detail. Also, the performance of the MMINs for the extraction of TC in the spiked pork sample was assessed.

2. Experimental

2.1. Materials

MAA, iron (III) chloride hexahydrate ($FeCl_3{\cdot}6H_2O$), sodium acetate (NaAc), ethylene glycol (EG), polyethylene glycol (PEG-1500), acetone, toluene, acetic acid (HAC) and HPLC-grade methanol were obtained from Sinopharm Chemical Reagent Co., Ltd. (Shanghai, China). Ethylene glycol dimethacrylate (EGDMA), CuCl, N,N,N′,N″,N″-pentamethyl diethyenetriamine (PMDETA), ethyl-2-bromoisobutyrate (EBiB), TC, sulfamethazine (SMZ), cefalexin (CEX), polyoxyethylene-(20) sorbitan monolaurate (Tween 20), and KH-570 from Aladdin Reagent Co., Ltd. (Shanghai, China) were used as received. Deionized ultrapure water was purified with a Purelab ultra (Organo, Tokyo, Japan).

2.2. Synthesis of functionalized Fe_3O_4 particles

Monodisperse Fe_3O_4 particles were synthesized according to the reported method [29]. The obtained Fe_3O_4 particles were then modified successively with KH-570 introduced polymerizable double bonds. Briefly, 0.5 g of the obtained magnetic nanospheres and 5.0 mL KH-570 were dispersed in 50 mL of dry toluene and stirred under nitrogen atmosphere at 50 °C for 12 h. The products were then collected and washed with toluene for several times. Finally, surface-modified magnetic particles (Fe_3O_4-KH570) dried under vacuum at room temperature.

2.3. Synthesis of magnetic TC-imprinted nanoparticles

The magnetic TC-imprinted nanoparticles were prepared via ATREP according to the following procedure: briefly, MAA (2.4 mmol), EGDMA (14.4 mmol), Fe_3O_4-KH570 (80 mg), tetracycline (0.03 mmol) were dissolved in 20 mL of water solution containing 0.3 g of Tween 20 in a round-bottom flask for prepolymerization at room temperature. The flask was deoxygenated for 30 min by exchanging with nitrogen. Then PMDETA (0.1 mmol) was added in to the solution, and CuCl (0.1 mmol) was also quickly transferred into the flask under the protection of nitrogen. The flask was immersed in an oil bath at 60 °C. Finally, the N_2-purged initiator EBiB (0.15 mmol) was injected into the reaction system. The reaction was allowed to proceed for 4.0 h, and then opened to air in order to stop polymerization. The resulting products were collected by magnetic field and washing thoroughly with water, ethanol and acetone to remove the unreacted monomers. Then the material was eluted extracted in a Soxhlet apparatus with a mixture of methanol/acetic acid (9.0/1.0, v/v) until no TC could be detected by UV–vis (at 280 nm) in the eluent. The obtained MMINs were finally dried under vacuum for 12 h before use.

Correspondingly, MNINs were prepared by the same procedure, but without using the template TC in the polymerization process.

2.4. Characterization of the nanoparticles prepared

Infrared spectra were recorded on a Nicolet NEXUS-470 FT-IR apparatus (U.S.A.). The morphology was observed by transmission electron microscope (TEM, JEOL IEM-200CX) and field-emission scanning electron microscope (FE-SEM, S-4800). Magnetic measurements were carried out using a VSM (7300, Lakeshore) under a magnetic field up to 10 kOe. The thermogravimetric analysis (TGA) of samples was measured using a Diamond TG/DTA instruments (STA 449C Jupiter, Netzsch, Germany) under a nitrogen atmosphere up to 800 °C with a heating rate of 5.0 °C min^{-1}. A TBS-990 atomic absorption spectrophotometer (Beijing Purkinje General Instrument Co. Ltd, Beijing, China) was used.

2.5. Batch rebinding experiment

To investigate the adsorption equilibrium of MMINs, 10 mg of MMINs was added into 10 mL of TC solution with initial concentrations varying from 10 mg L^{-1} to 300 mg L^{-1} without any pH adjustment. After 12 h, the saturated polymers were separated by an external magnet. The supernatants were then filtered with sterile 0.2 μm filter units before being sent for High performance liquid chromatograph (HPLC) analysis. An HPLC system (Agilent 1200 series, U.S.A.) was equipped with a UV–vis detector (set at 280 nm). The injection loop volume was 20 μL. The mobile phase consisted of deionized ultrapure HAC water solution (pH 3) and methanol at a volume ratio of 70:30 with a flow rate of 1.0 mL min^{-1}, and the oven temperature was set at 25 °C. The equilibrium adsorption amounts of TC were calculated according to the following equation:

$$Q_e = \frac{(C_0 - C_e)V}{m} \tag{1}$$

where Q_e (mg g^{-1}) is the amount of TC adsorbed at equilibrium, C_0 and C_e (mg L^{-1}) are the concentrations of TC at initial and equilibrium, respectively. V is the volume of TC solution, and m is the weight of MMINs.

The adsorption kinetics studies were identical with those of equilibrium tests, the initial concentration was set as 50 mg L^{-1}, and the samples were separated at predetermined time intervals. The amount of TC adsorbed (Q_t, mg g^{-1}) was calculated according to the following equation:

$$Q_t = \frac{V(C_0 - C_{t})}{m} \tag{2}$$

where C_t (mg L^{-1}) is the concentration of TC solution at any time t.

To investigate the selectivity of the MMINs, 10 mg of the MMINs/MNINs were added into test tubes, each of which contained 10 mL solution with 30 mg L^{-1} of TC, OTC, SMZ and CEX, respectively. At the same time, the competitive sorption of the MMINs/MNINs for TC at the presence of 30 mg L^{-1} of OTC, SMZ and CEX was studied. The initial solution pH was not adjusted and the experiments were carried out at 25 °C for 6.0 h.

2.6. Magnetite leakage studies

In order to determine the leaking amount of magnetite from the MMINs, 100 mg of the MMINs were placed in the test tubes containing 10 mL of distilled water with different pH ranging from 2.0 to 9.0, and were shaken for 12 h. The amount of the iron ions leaked was determined by a graphite furnace atomic absorption spectrophotometer.

2.7. Pork sample preparation and solid phase extraction (SPE) procedure

10 g of pork was minced and mixed into 50 mL of 5.0% trichloroacetic acid aqueous solution. The sample was extracted by ultrasonic agitation for 30 min. After being centrifuged at 4000 rpm for 15 min, the supernatant was filtered through a 0.22 μm filter and stored at 4 °C for the SPE procedure.

50 mg of MMINs was put into a tube containing 5.0 mL of the sample with the spike concentration of 50 μg L^{-1}, and the mixture was shaken for 6.0 h at room temperature. Subsequently, the MMINs with adsorbed TC were separated rapidly by an adscititious magnet. Then the supernatant was discarded and the MMINs were washed with acetonitrile twice. Finally, TC was eluted from the MMINs (also MNINs) with 10 mL of methanol solution containing 5.0% acetic acid and then evaporated to dryness at 40 °C under nitrogen. The residues were dissolved with 1.0 mL of 20% aqueous methanol for further HPLC analysis.

3. Results and discussion

3.1. Preparation of the MMINs

This work focused on the application of ATREP in the preparation of magnetic TC-imprinted nanoparticles. Fig. 1 illustrated the synthesis routes of magnetic TC-imprinted nanoparticles. Firstly, the Fe_3O_4 particles were prepared by the thermal decomposition of iron (III) chloride hexahydrate with the aid of EG and PEG, which possessed of a high crystallinity and narrow size distribution [29], and the pure Fe_3O_4 particles tended to form large aggregates in aqueous solution. However, after the surface modification with KH-570, magnetic particles could inhibit the formation of aggregates to certain extent and prevented oxidation of Fe_3O_4 [30]. Moreover, vinyl functional monomers were immobilized at the surface of Fe_3O_4 nanoparticles can take part in the free radical polymerization, which can avoid leakage of Fe_3O_4 particles.

Subsequently, MAA was chosen as functional monomer based on the consideration that the carboxylic group of MAA and hydroxyl, amine and amide groups of TC could provide multiple hydrogen-binding sites. Here, the mol ratio of template and monomer was chosen 1:8 according to the former work [31]. EGDMA as a cross-linking agent was chosen to participate in the polymerization reaction. The polymerization was initiated by the initiating radicals, which were stemmed from the reaction between an alkyl halide (EBiB) and a transition metal complex (Cu^+/PMDETA) in its lower oxidation state. The equilibrium between the dormant species (alkyl halides) and active species (radicals) can be quickly established soon after the polymerization started, which was crucial for achievement of the controlled polymerization [32]. The atom transfer radical polymerization was carried out in an emulsion system containing water and surfactant (Tween 20), and the imprinted particles were in nano-scale as expected. Moreover, the ATREP time of 4.0 h at 60 °C was chosen for the preparation of the MMINs [33].

3.2. Characterization of the MMINs

SEM and TEM were used to capture the microscopic images of the particles prepared. As shown in Fig. 2c, highly monodispersed and spherical Fe_3O_4 particles were synthesized. It can be seen that uniform size of the particles was around 200 nm, which was basically consistent with the work by Deng et al. [29]. For the MMINs, the SEM images (shown in Fig. 2a and b) revealed two different particles with size ranges from 80 to 100 nm and from 300 to 600 nm, respectively. The same result was also can be obtained in Fig. 2d. The smaller nanoparticles should be the product of co-polymerization of MAA and EGDMA, and the bigger particles were Fe_3O_4 particles coated by molecular imprinted polymer layers with the thickness ranging from 50 to 200 nm by calculation. The nanoparticles were crosslinked to form three-dimensional net and grafted onto the surface of bigger particles, which shared the magnetic susceptibility and lead to the decrease in the saturation magnetization of the whole MMINs matching with the results of the VSM. The majority of the particles were approximately spherical, and the surface of particles was porous and rough, which may be caused by the removal of template molecule and surfactant and be favor of rebinding or

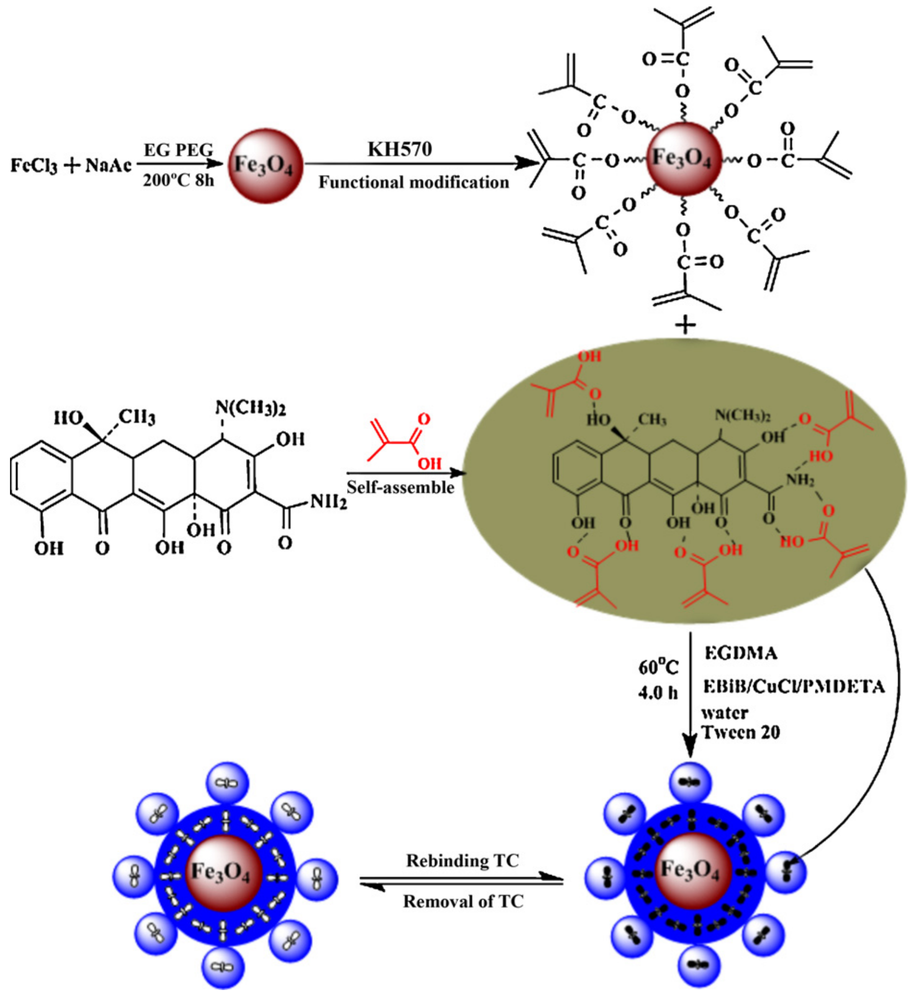

Fig. 1. Schematic representation of the possible process of the MMINs.

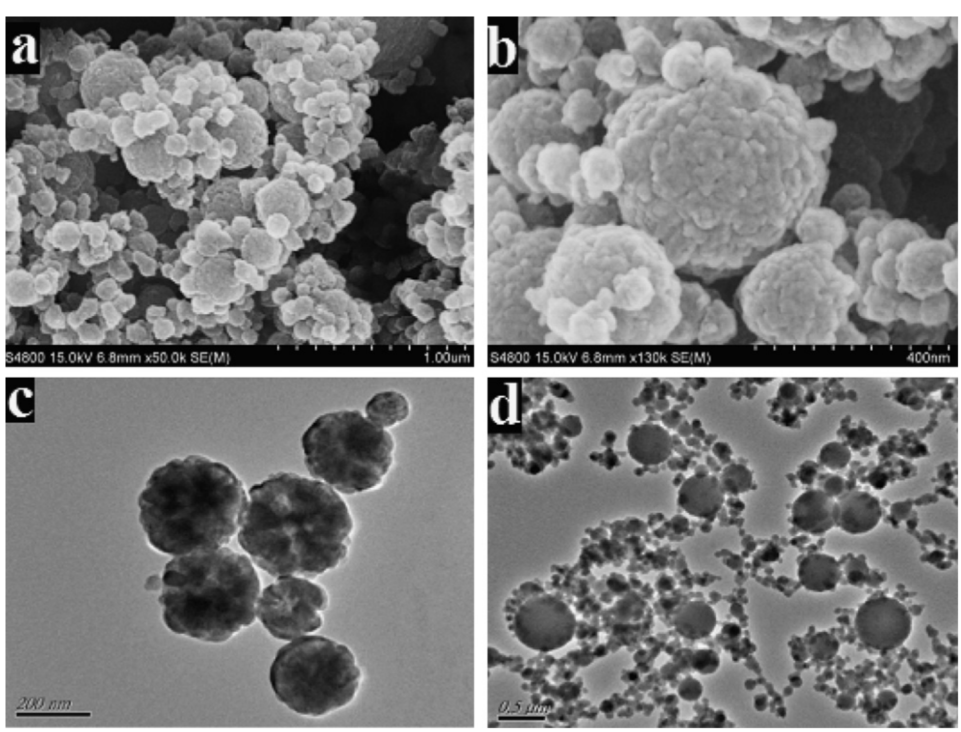

Fig. 2. SEM images of the MMINs with different magnification of 50 K (a) and 130 K (b); TEM images of the Fe_3O_4 nanoparticles (c) and MMINs (d).

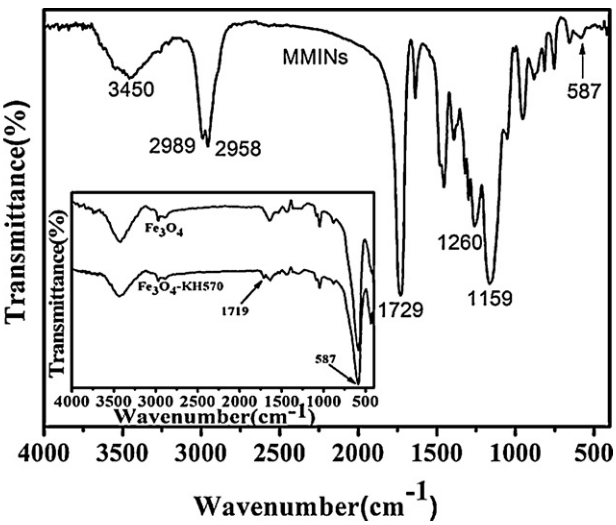

Fig. 3. FT-IR spectra of the bulk Fe_3O_4, Fe_3O_4-KH570 (inset) and MMINs.

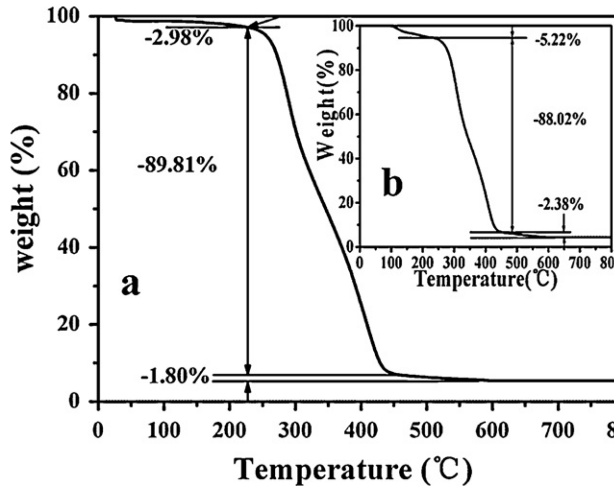

Fig. 4. Thermogravimetric analysis of the MMINs (a) and MNINs (b).

releasing the target molecules. There were no significant differences between the morphology of MMINs and MNINs (not shown). The presence of the template molecule during the polymerization had slight influence on the morphology of resulting product, as has been observed in the other reaction system for preparing molecularly imprinted nanoparticles [34].

The FT-IR spectroscopy of the bared, KH570-modified Fe_3O_4 and MMINs was measured and shown in Fig. 3, respectively. The corresponding infrared absorption peaks can confirm the main functional groups of the predicted structure. A distinct absorption band at 587 cm^{-1} attributed to Fe—O bond in the spectrum of Fe_3O_4 nanoparticles, which was also obtained for Fe_3O_4-KH570 and MMINs. Meanwhile, the strength of Fe—O stretching decreased, due to the coated polymer shells on the surface of the Fe_3O_4 nanoparticles, which clearly confirmed the above polymerization process. Compared with the infrared data of bare Fe_3O_4, the KH570-modified Fe_3O_4 nanoparticles displayed the characteristic peak of carbonyl group at 1729 cm^{-1} marked by the arrow, which confirmed that vinyl groups were successfully introduced to the surface of the Fe_3O_4 nanoparticles via the silanization reaction [35]. A broad absorption band at 3450 cm^{-1} of the MMINs corresponded to the stretching vibration of O—H bonds of the hydroxyl groups for MAA molecules. The typical absorption bands of MMINs were at 2989 and 2958 cm^{-1} assigned to the C—H asymmetry stretching vibrations of both —CH_3 and —CH_2 groups. The C—O symmetric and asymmetric stretching vibration bands of ester (EGDMA) were around 1260 and 1159 cm^{-1}, respectively [36]. In addition, the small C═C stretching vibration peaks around 1637 cm^{-1} demonstrated that the bonds of EGDMA molecules were not 100% crosslinked in the MMINs [37]. All the results revealed that the co-polymerization using ATREP was successfully achieved.

TGA was performed to further quantify the amount of Fe_3O_4 encapsulated in the magnetic polymer matrix. As shown in Fig. 4, the thermogravimetric analysis (TGA) of MMINs and MNINs have a similar general shape composing of three stage of mass change from room temperature to 800 °C. The first stage occurred from room temperature to 240 °C, the decrease of weight were 2.98% and 5.22% for MMINs and MNINs, respectively, which may due to the dehydration of the water residues in the polymer. The onset temperature of thermal decomposition was relatively close to that obtained in similar studies done by Tan et al. [38]. Significant mass loss in the second stage started from 240 to 450 °C, which was caused by the loss of imprinted polymers. In this stage, there were no significant differences between the MMINs and MNINs, the value of the mass loss were 89.81% and 88.02%, respectively. The mass remained relatively constant for the rest of the analysis from 450 to 800 °C. The remnant was attributed to the more thermally resistant Fe_3O_4 magnetite, thus giving a magnetite encapsulation efficiency of 5.41 wt%. The obtained encapsulation efficiency was relatively high and satisfactory when compared to those from previous works [39,40], where the content of Fe_3O_4 averaged only 2.0–4.0 wt%. Similar magnetite encapsulation efficiency of 4.38 wt% was obtained for MNINs, indicating the MMINs and MNINs possessed of a similar degree of polymerization.

The magnetic properties of Fe_3O_4, MMINs and MNINs were investigated with a VSM. Fig. 5a and b showed the magnetization curves of three samples were no hysteresis and symmetrical about the origin, suggesting that the samples were superparamagnetic, which facilitated magnetic separation and reusability. The saturation magnetization (*Ms*) values obtained at room temperature were 78.63 emu g^{-1}, 1.68 emu g^{-1} and 1.53 emu g^{-1}, respectively. This result agreed with the experiments of thermogravimetric analysis. The decrease in magnetization value was expected because the polymeric coating had effectively shielded the magnetite. However, the MMINs with less magnetite encapsulation also possess enough magnetic response to meet the need of magnetic separation quickly, as shown in Fig. 5d. Magnetic responsive experimental phenomena was that a brown homogeneous dispersion without the external magnetic field; when the present of the external magnetic field, the brown particles were attracted to the wall of vial with the solution turning to be transparent and clear. The results also illustrated that MMINs was a feasible magnetic separation carrier. In Fig. 5c, magnetite leakage study exhibited that extremely small amount of iron ion was detected in the solutions with different pH. And 20 μg was leaked from 100 mg of MMINs even at pH 2.0, which is only 0.02% by weight, suggesting that the mean prevented magnetite leakage successfully.

3.3. Adsorption isotherms

To evaluate the adsorption capacity of the MMINs for TC and the equilibrium constants, the absorption isotherm experiments for were performed at the different TC concentrations ranging from 10 to 300 mg L^{-1}. As shown in Fig. 6, the amount of absorbed TC per unit mass of the nanoparticles increased in the whole concentration range, while the MMINs exhibited the higher adsorption capacity compared with the MNINs. The recognition sites on the surface and in the proximity of imprinted nanoparticles' surface displayed better steric matching with the imprinted molecules, which could

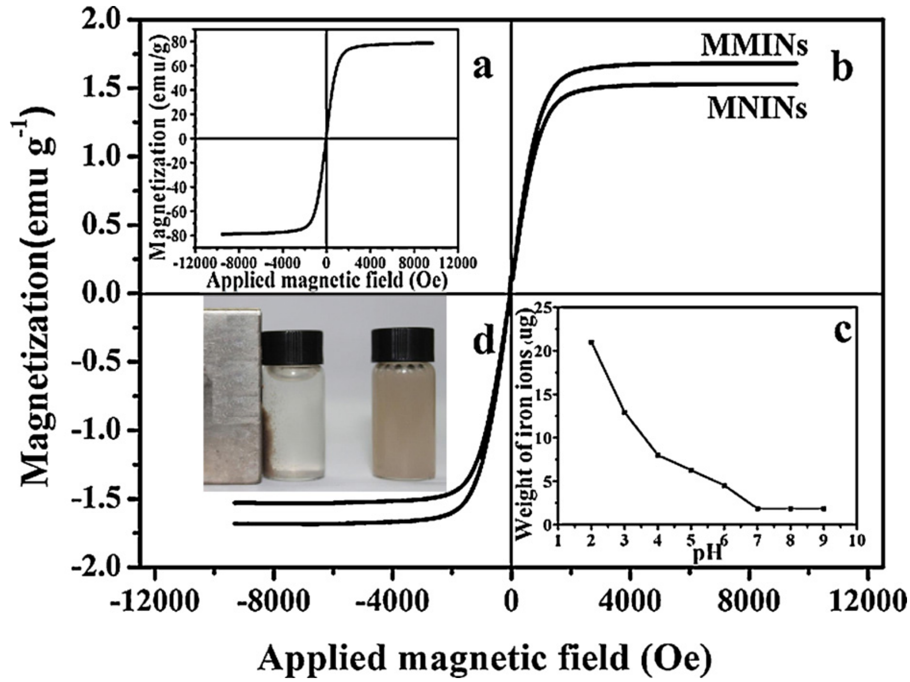

Fig. 5. Magnetization curves obtained by VSM at room temperature of Fe_3O_4 (a), MMINs and MNINs (b); magnetite leakage curve of the MMINs (c) and A photograph of MMINs dispersed in the water in the presence (left) and absence (right) of an external magnetic field (d).

capture more TC. Here, Langmuir isotherm model was used to analysis experimental data. The nonlinear expression of the Langmuir model [41] was given by Eq. (3)

$$Q_e = \frac{K_L Q_m C_e}{1 + K_L C_e} \quad (3)$$

where Q_e (mg g^{-1}) is the equilibrium amount of TC adsorbed by the polymeric nanoparticles, C_e (mg L^{-1}) the equilibrium concentration of adsorbate, Q_m (mg g^{-1}) is the saturation adsorption capacity and K_L (L mg^{-1}) is the Langmuir constant.

The regression curves of Langmuir model for MMINs and MNINs were obtained in Fig. 6, and the involved parameters were shown in Table 1. The results of regression (R^2 values above 0.97) illustrated Langmuir isotherm fitted quite well with the experimental data. The calculated maximum monolayer adsorption capacities of MMINs and MNINs were 12.10 mg g^{-1} and 1.80 mg g^{-1}, respectively. The imprinting factor estimated was 6.33, which suggested that the MMINs exhibited high specific adsorption for TC molecules. The results demonstrated that the active sites distribution of MMINs and MNINs was homogeneous profiting from ATREP.

Table 1
Langmuir adsorption isotherm constants for TC onto the MMINs and MNINs.

Adsorbents	$Q_{e,exp}$ (mg g^{-1})	$Q_{e,c}$ (mg g^{-1})	K_L (L mg^{-1})	R^2
MMINs	12.51	14.31	0.0191	0.9953
MNINs	1.99	2.26	0.0355	0.9783

3.4. Adsorption kinetics

Fig. 7 shows the adsorption kinetics spots of TC on MMINs and MNINs from aqueous solution containing 50 mg L^{-1} TC with various contact times. The TC adsorption was observed to rapid increase in the first 100 min, which was attributed to the presence of a large

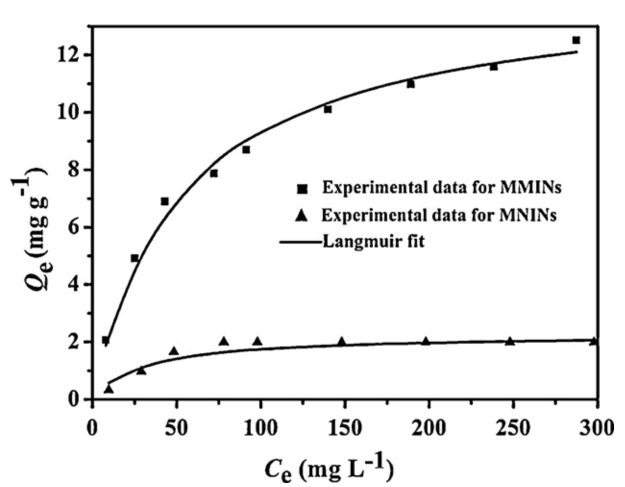

Fig. 6. Adsorption isotherms of TC on the MMINs and MNINs with the fitting to Langmuir model.

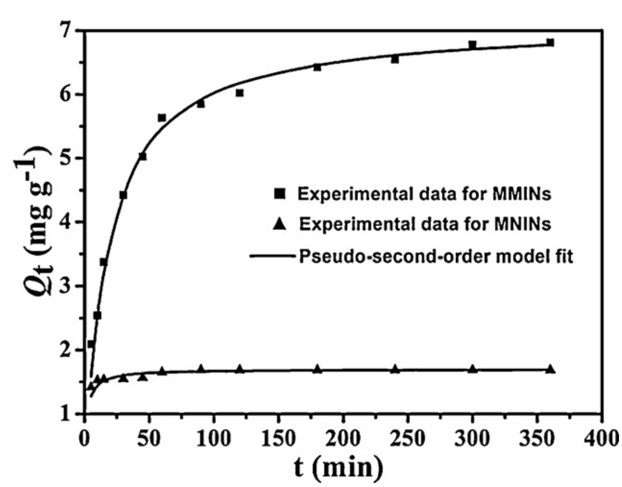

Fig. 7. Adsorption dynamic curves of TC on the MMINs and MNINs with the fitting to pseudo-two-order model.

Table 2
Kinetics constants for the pseudo-first-order and pseudo-second-order rate equations.

	The pseudo-first-order model				The pseudo-second-order model		
Adsorbents	$Q_{e,exp}$ (mg g^{-1})	$Q_{e,c}$ (mg g^{-1})	k_1 (min^{-1})	R^2	$Q_{e,c}$ (mg g^{-1})	k_2 (g mg^{-1} min^{-1})	R^2
MMINs	6.810	4.128	0.0144	0.9461	7.102	0.0081	0.9995
MNINs	1.686	1.997	0.0565	0.8278	1.697	0.3607	0.9999

amount of empty, high-affinity binding sites on the surface of the particles enabled template TC to easily rebind with less mass resistance. In the subsequent step, when TC filled up most of the binding sites, the equilibrium was slowly achieved.

To investigate the rate-controlling mechanism of adsorption processes such as mass transfer and chemical reaction, the kinetic data obtained from batch experiments was fitted with the pseudo-first-order [42] and pseudo-second-order rate equations [43]. The pseudo-first-order model can be expressed as follows:

$$Q_t = Q_e - Q_e e^{-k_1 t} \quad (4)$$

where Q_e and Q_t (mg g^{-1}) are the amounts of TC molecular adsorbed onto adsorbent at equilibrium and any time t, respectively. k_1 (min^{-1}) is the first-order rate constant.

The pseudo-two-order model can be expressed as Eq. (5):

$$Q_t = \frac{k_2 {Q_e}^2 t}{1 + k_2 Q_t t} \quad (5)$$

where k_2 is the second-order rate constant.

The adsorption kinetics constants and linear regression values of the two models were listed in Table 2, and the nonlinear regression of the pseudo-second-order rate equation for TC rebinding was shown in Fig. 6. The pseudo-first-order model exhibited relatively poor fitting with low regression coefficients value (R^2) and variance between the experimental and theoretical values. The adsorption of TC obeyed pseudo-second-order rate equation well because of the favorable agreement between experimental and calculated values of Q_e (R^2 values above 0.99). The results suggested that the pseudo-second-order mechanism was predominant and that chemisorption may be the rate-limiting step that controlled the adsorption process for TC [44].

3.5. Selectivity of the MMINs

To investigate the rebinding selectivity of the prepared MMINs towards TC molecule, OTC, CEX, and SMZ were selected as the structural analogue and reference antibiotics with different molecular structure, respectively. The adsorption experiments for each adsorbate were carried out under the same condition and the rebinding capacities of the MMINs and MNINs for these antibiotics were determined using the equilibrium adsorption method with a feed concentration of 30 mg L^{-1}, as shown in Fig. 8. The MMINs exhibited higher capacity for TC compared with CEX and SMZ, indicating higher rebinding selectivity for TC, which was attributed to the molecular size recognition. However, the uptake of OTC onto MMINs was nearly the same as TC, due to almost the same molecule structure. Fig. 8 clearly exhibited that the rebinding capacity of MMINs towards the four adsorbates was greatly higher than MNINs, which was attributed to the interactions between functional groups of the targets and imprinted cavities. During the preparation of MMINs, hydrogen interaction between the carboxylic group of MAA and hydroxyl, amine and amide groups of TC was involved in the monomer–template interaction, which played an important role in the recognition during the adsorption process. The selective adsorption process was complex, besides the hydrogen interaction, others interactions may also be involved.

To further probe the molecular rebinding selectivity of the MMINs for TC, three competitive antibiotics (OTC, CEX and SMZ)

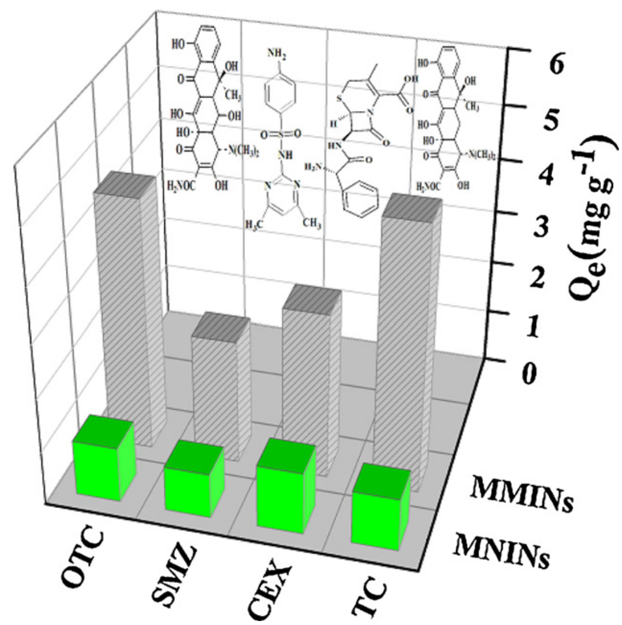

Fig. 8. Adsorption capacities for the template TC and other antibiotics.

were added into TC solution to determine their interference in TC adsorption. The MMINs and MNINs were exposed to the binary system with an initial concentration of 30 mg L^{-1}, respectively. As shown in Fig. 9, The MMINs still displayed high TC adsorption capacity in the presence of other antibiotics. When OTC was present in the TC solution, the adsorption capacity of TC onto MMINs decreased almost a half (from 4.91 mg g^{-1} to 2.70 mg g^{-1}) as expected. Because of the presence of an additional competitive antibiotic in the binary system, the TC uptake for the MMINs

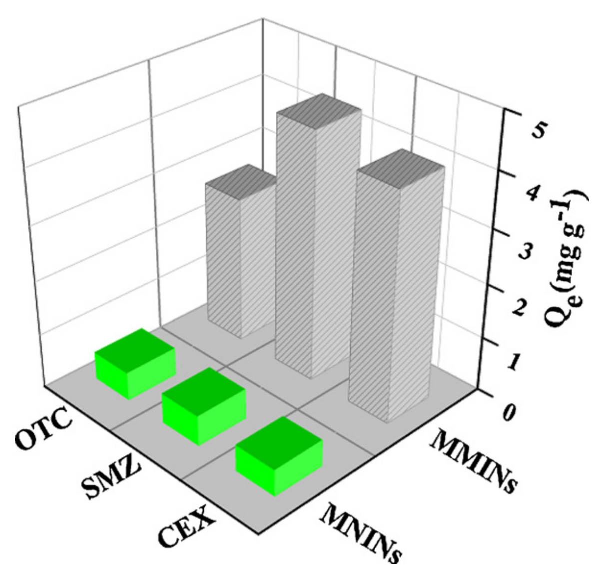

Fig. 9. Adsorption selectivity of TC onto the MMINs and MNINs in dual-solute solution in the presence of competitive antibiotics.

Table 3
Comparison of the TC-MIPs prepared before to this paper described.

Authors	Methodology	Time (*h*)	Solvent	Q_m	*I*	Reference
Hu et al.	Multiple co-polymerization	24	Toluene	77.6 pmol/4 cm	3.9	[45][b]
Caro et al.	Bulk polymerization	24	Acetonitrile	No report	4.0	[31][b]
Cai and Gupta	Bulk polymerization	24	Acetonitrile	3.8 mg g^{-1}	No report	[46][a]
Suedee et al.	Bulk polymerization	18	Water Acetonitrile	2.96 μmol g^{-1-1} 0.98 μmol g	1.74 1.92	[47][a]
Wang et al.	Precipitation polymerization	24	Water	73 μmol g^{-1}	1.80	[48][a]
This paper	ATREP	4.0	Water	27.2 μmol g^{-1}	6.33	This paper[a]

Q_m is the maximum adsorption capacity; *I* is the imprinting factor.
[a] IF value obtained under equilibrium condition.
[b] IF value obtained under chromatographic (non-equilibrium) condition.

had slightly decreased as compared to that for the single system, but the differences in the adsorption capacity of TC between the MMINs and MNINs were more obvious, indicating higher selectivity in binary solution. In contrast, the MNINs were affected significantly by the competitive antibiotic. The results illustrated the high TC-imprinting efficiency achieved through ATREP.

3.6. Comparison of TC-MIPs with existing reports

Several literatures for preparation of MIPs using TC as the template have been published, which were summarized in Table 3. Hu et al. [45] reported a novel MIP-coated solid-phase microextraction (SPME) fiber for trace analysis of TCs in complicated samples, but the extraction capacity towards TC was only 3.9 times as much as the NIP-coated fiber. Caro et al. [31], Cai and Gupta [46] and Suedee et al. [47] prepared the MIPs using bulk polymerization, which was tedious, time consuming and the prepared particles showed an irregular shape and size. In addition, all of the MIPs showed very low capacity and imprinting factor. Wang et al. [48] prepared hydrophilic MIPs using TC as template by precipitation polymerization. Although the adsorption capacity of hydrophilic MIPs was 73.0 μmol g^{-1} in water medium, which was significantly improved, the imprinting factor was just 1.80. In our study, ATPEP was adopted for the preparation of MMINs, which not only had high adsorption capacity (27.2 μmol g^{-1}) and imprinting factor (6.33) in water medium, but also shortened the time of polymerization, which exhibited the tremendous advantage and may propose a thinking to achieve the selective recognition of the target molecule in aqueous environmental samples.

3.7. Regeneration of MMINs and potential practical application

To test the stability and regeneration of the MMINs, five (adsorption/desorption) regeneration cycles were conducted with TC. The mixture of methanol and acetic acid (9.0:1.0, V/V) was used as an eluent. After the supernatant solution was discarded, the MMINs were dipped in 10 mL of eluent under the ultrasound for 30 min. The adsorption results were shown in Fig. 10. After five cycles of regeneration, the adsorption capacity of MMINs for TC was about 6.48% loss, suggesting good retention of the activity of the MMINs.

To demonstrate the applicability of the method, real sample of pork was analyzed. The samples spiked with 50 μg L^{-1} TC was extracted by the MMINs and MNINs, and the chromatogram was illustrated in Fig. 11. The MNINs apparently lacked specific enrichment properties to the target TC, which could not be detected by HPLC. By contrast, the high selectivity was observed for the MMINs owing to the special recognition to the template molecule. The recovery was 78.1% for the spiked pork sample with the RSD of 6.6% (n = 5). The results indicated that the proposed MMINs had good applicability to selective extraction of TC from complex samples.

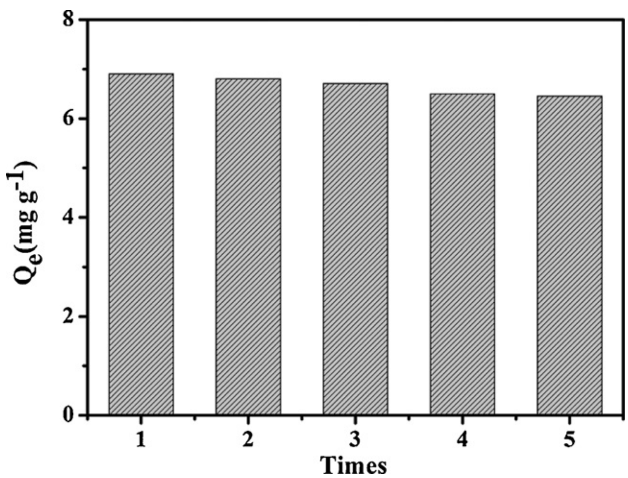

Fig. 10. Stability and potential regeneration of the MMINs.

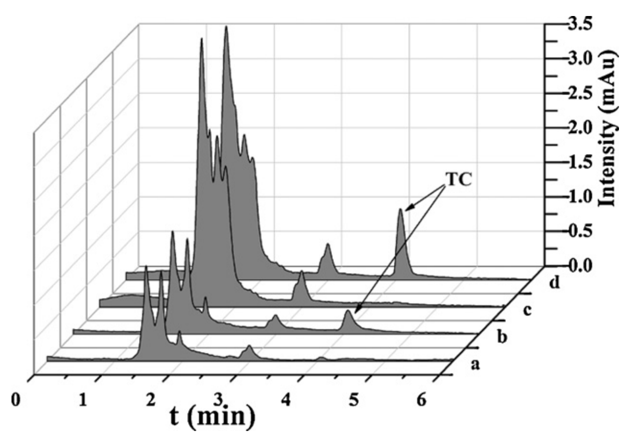

Fig. 11. Chromatograms of TC in pork sample with UV detection. 5.0% $HClO_4$ extracted sample solution (a), TC spiked sample solution with 50 μg L^{-1} TC (b), spiked sample solution extracted with the MNINs (c) and with the MMINs (d).

4. Conclusions

In this work, a novel molecularly imprinted nanotechnique for the selective recognition and removal of TC in aqueous solution combing ATRP and emulsion polymerization were proposed. Using this technique, the time of polymerization was dramatically shortened as compared to that by conventional radical polymerization. The prepared magnetic molecularly imprinted nanoparticles exhibited good characteristics such as excellent specific recognition, and adsorption capacity and thermal stability. The Fe_3O_4 nanoparticles were modified with KH-570 and then used as magnetically susceptible monomer participating in the polymerization. Characterization of the magnetic properties showed that sufficient Fe_3O_4 nanoparticles were encapsulated and the MMINs displayed the desired superparamagnetic susceptibility. The method not only avoided the leakages of Fe_3O_4 particles but also lead to a fast and selective recognition of TC from aqueous solutions. The prepared MMINs also exhibited the excellent property of regeneration. We believe that ATREP is a powerful technique to prepare molecularly imprinted nanoparticles for various applications such as environmental pollutants separation, recognition elements in biosensors and drug delivery.

Acknowledgments

This work was financially supported by the National Natural Science Foundation of China (nos. 21077046, 21107037, 21176107, and 21174057), Ph.D. Programs Foundation of Ministry of Education of China (no. 20093227110015), Ph.D. Innovation Programs Foundation of Jiangsu Province (no. CX10B_276Z) and Natural Science Foundation of Jiangsu Province (no. SBK201122883).

References

[1] A.D. Cooper, G.W.F. Stubbings, M. Kelly, J.A. Tarbin, W.H.H. Farrington, G. Shearer, Improved method for the on-line metal chelate affinity chromatography–high-performance liquid chromatographic determination of tetracycline antibiotics in animal products, J. Chromatogr. A 812 (1998) 321–326.

[2] B. Halling-Sørensen, G. Sengeløv, J. Tjørnelund, Toxicity of tetracyclines and tetracycline degradation products to environmentally relevant bacteria, including selected tetracycline resistant bacteria, Arch. Environ. Contam. Toxicol. 42 (2002) 263–271.

[3] A.B.A. Boxall, D.W. Kolpin, B. Halling-Sørensen, J. Tolls, Are veterinary medicines causing environmental risks? Environ. Sci. Technol. 37 (2003) 286A–294A.

[4] D.S. Aga, S. O'connor, S. Ensley, J.O. Payero, D. Snow, D. Tarkalson, Determination of the persistence of tetracycline antibiotics and their degradates in manure-amended soil using enzyme-linked immunosorbent assay and liquid chromatography–mass spectrometry, J. Agric. Food Chem. 53 (2005) 7165–7171.

[5] A.L. Batt, D.S. Aga, Simultaneous analysis of multiple classes of antibiotics by ion trap LC/MS/MS for assessing surface water and groundwater contamination, Anal. Chem. 77 (2005) 2940–2947.

[6] K.De Wasch, L. Okerman, S. Croubels, H.De Brabander, J. VanHoof, P.De Backer, Detection of residues of tetracycline antibiotics in pork and chicken meat: correlation between results of screening and confirmatory tests, Analyst 123 (1998) 2737–2741.

[7] H. De Ruyck, H. De Ridder, Determination of tetracycline antibiotics in cow's milk by liquid chromatography/tandem mass spectrometry, Rapid Commun. Mass Spectrom. 21 (2007) 1511–1520.

[8] G. Alfredsson, C. Branzell, K. Granelli, A. Lundstrom, Simple and rapid screening and confirmation of tetracyclines in honey and egg by a dipstick test and LC-MS/MS, Anal. Chim. Acta 529 (2005) 47–51.

[9] H.M. Thompson, R.J. Waite, S. Wilkins, M.A. Brown, T. Bigwood, M. Shaw, Effects of European foulbrood treatment regime on oxytetracycline levels in honey extracted from treated honeybee (*Apis mellifera*) colonies and toxicity to brood, Food Addit. Contam. 22 (2005) 573–578.

[10] A.L. Cinquina, F. Longo, G. Anastasi, L. Giannetti, R. Cozzani, Validation of a high-performance liquid chromatography method for the determination of oxytetracycline, tetracycline, chlortetracycline and doxycycline in bovine milk and muscle, J. Chromatogr. A 987 (2003) 227–233.

[11] G. Wulff, Molecular imprinting in cross-linked materials with the aid of molecular templates—a way towards artificial antibodies, Angew. Chem. Int. Ed. 34 (1995) 1812–1832.

[12] J.L. Urraca, M.C. Moreno-Bondi, A.J. Hall, B. Sellergren, Direct extraction of Penicillin G and derivatives from aqueous samples using a stoichiometrically imprinted polymer, Anal. Chem. 79 (2007) 695–701.

[13] R. Sancho, C. Minguillón, The chromatographic separation of enantiomers through nanoscale design, Chem. Soc. Rev. 38 (2009) 797–805.

[14] N. Kirsch, J.P. Hart, D.J. Bird, R.W. Luxton, D.V. Mccalley, A new electrochemical enzyme-linked immunosorbent assay for the screening of macrolide antibiotic residues in bovine meat, Analyst 126 (2001) 1936–1941.

[15] P. Pasetto, S.C. Maddock, M. Resmini, Synthesis and characterisation of molecularly imprinted catalytic microgels for carbonate hydrolysis, Anal. Chim. Acta 542 (2005) 66–75.

[16] J.M. Pan, X.H Zou, X. Wang, W. Guan, Y.S Yan, J. Han, Selective recognition of 2,4-dichlorophenol from aqueous solution by uniformly sized molecularly imprinted microspheres with β-cyclodextrin/attapulgite composites as support, Chem. Eng. J. 162 (2010) 910–918.

[17] A. Beltran, F. Borrull, P.A.G. Cormack, R.M. Marce, Molecularly-imprinted polymers: useful sorbents for selective extractions, TrAC, Trends Anal. Chem. 29 (2010) 1363–1375.

[18] D. Gao, Z. Zhang, M. Wu, C. Xie, G. Guan, D. Wang, A surface functional monomer-directing strategy for highly dense imprinting of TNT at surface of silica nanoparticles, J. Am. Chem. Soc 129 (2007) 7859–7866.

[19] Y.C. Lin, H.H. Pan, C.C. Hwang, W.C. Lee, Side chain functionality dominated the chromatography of N-protected amino acid on molecularly imprinted polymer, J. Appl. Polym. Sci. 105 (2007) 3519–3524.

[20] K. Haupt, K. Mosbach, Molecularly imprinted polymers and their use in biomimetic sensors, Chem. Rev. 100 (2000) 2495–2504.

[21] B.Y. Zu, G.Q. Pan, X.Z. Guo, Y. Zhang, H.Q. Zhang, Preparation of molecularly imprinted polymers via atom transfer radical "bulk" polymerization, J. Polym. Sci. Part A: Polym. Chem. 48 (2010) 532–541.

[22] X. Wei, S.M. Husson, Surface-grafted molecularly imprinted polymers grown from silica gel for chromatographic separations, Ind. Eng. Chem. Res. 46 (2007) 2117–2124.

[23] X. Wei, S.M. Husson, Surface molecular imprinting by atom transfer radical polymerization, Biomacromolecules 6 (2005) 1113–1121.

[24] X. Li, S.M. Husson, Adsorption of dansylated amino acids on molecularly imprinted surfaces: a surface plasmon resonance study, Biosens. Bioelectron. 22 (2006) 336–348.

[25] S. Gam-Derouich, a M.N. Nguyen, A. Madani, N. Maouche, P. Lang, C. Perruchot, M.M.Chehimi, Aryl diazoniumsalt surface chemistry and ATRP for the preparation of molecularly imprinted polymer grafts on gold substrates, Surf. Interface Anal. 42 (2010) 1050–1056.

[26] C.H. Lu, Y. Wang, Y. Li, H.H. Yang, X. Chen, X.R. Wang, Bifunctional superparamagnetic surface molecularly imprinted polymer core–shell nanoparticles, J. Mater. Chem. 19 (2009) 1077–1079.

[27] H.J. Wang, W.H. Zhou, X.F. Yin, Z.X. Zhuang, H.H. Yang, X.R. Wang, Template synthesized molecularly imprinted polymer nanotube membranes for chemical separations, J. Am. Chem. Soc. 128 (2006) 15954–15955.

[28] B.Y. Zu, G.Q. Pan, X.Z. Guo, Y. Zhang, H.Q. Zhang, Preparation of molecularly imprinted polymer microspheres via atom transfer radical precipitation polymerization, J. Polym. Sci., Part A: Polym. Chem. 47 (3257–3270) (2009).

[29] H. Deng, X.L. Li, Q. Peng, X. Wang, J.P. Chen, Y.D. Li, Monodisperse magnetic singlecrystal ferrite, Angew. Chem. Int. Ed. 44 (2005) 2782–2785.

[30] T.Y. Chen, Z. Cao, X.L. Guo, J.J. Nie, J.T. Xu, Z.Q. Fan, B.Y. Du, Preparation and characterization of thermosensitive organic-inorganic hybrid microgels with functional Fe_3O_4 nanoparticles as crosslinker, Polymer 52 (2011) 172–179.

[31] E. Caro, R.M. Marcĕ, P.A.G. Cormack, D.C. Sherrington, F. Borrull, Synthesis and application of an oxytetracycline imprinted polymer for the solid-phase extraction of tetracycline antibiotics, Anal. Chim. Acta 552 (2005) 81–86.

[32] K. Matyjaszewski, J. Xia, Atom transfer radical polymerization, Chem. Rev. 101 (2001) 2921–2990.

[33] S. Jousset, J. Qiu, K. Matyjaszewski, Atom transfer radical polymerization of methyl methacrylate in water-borne system, Macromolecules 34 (2001) 6641–6648.

[34] C.J. Tan, S. Wangrangsimakul, R. Bai, Y.W. Tong, Defining the interactions between proteins and surfactants for nanoparticle surface imprinting through miniemulsion polymerization, Chem. Mater 20 (2008) 118–127.

[35] B.Y. Du, A.X. Mei, P.J. Tao, B. Zhao, Z. Cao, J.J. Nie, Poly[N-isopropylacrylamide-co-3(trimethoxysilyl)-propylmethacrylate] coated aqueous dispersed thermosensitive Fe_3O_4 nanoparticle, J. Phys. Chem. C 113 (2009) 10090–10096.

[36] K. Yoshimatsu, K. Reimhult, A. Krozer, K. Mosbach, K. Sode, L. Ye, Uniform molecularly imprinted microspheres and nanoparticles prepared by precipitation polymerization: the control of particle size suitable for different analytical applications, Anal. Chim. Acta 584 (2007) 112–121.

[37] I. Koprinarov, A.P.Hitchcock, W.H. Li, Y.M. Heng, H.D.H. Stöver, Quantitative compositional mapping of core–shell polymer microspheres by soft X-ray spectromicroscopy, Macromolecules 34 (2001) 4424–4429.

[38] C.J. Tan, H.G. Chua, K.H. Ker, Y.W. Tong, Preparation of bovine serum albumin surface-imprinted submicrometer particles with magnetic susceptibility through core shell miniemulsion polymerization, Anal. Chem. 80 (2008) 683–692.

[39] S. Lu, G. Cheng, X. Pang, Preparation of molecularly imprinted Fe_3O_4/P(St-DVB) composite beads with magnetic susceptibility and their characteristics of molecular recognition for amino acid, J. Appl. Polym. 89 (2003) 3790–3796.

[40] S. Lu, G. Cheng, X. Pang, Protein-imprinted soft-wet gel composite microspheres with magnetic susceptibility. II. Characteristics, J. Appl. Polym. 99 (2006) 2401–2407.

[41] I. Langmuir, The adsorption of gases on plane surfaces of glass, mica and platinum, J. Am. Chem. Soc. 40 (1918) 1361–1403.

[42] Y.S. Ho, G. McKay, The sorption of lead (II) ions on peat, Water Res. 33 (1999) 578–584.

[43] Y.S. Ho, G. McKay, Pseudo-second order model for sorption processes, Process Biochem. 34 (1999) 451–465.

[44] G. Baydemir, M. Andac, N. Bereli, R. Say, A. Denizli, Selective removal of bilirubin from human plasma with bilirubin-imprinted particles, Ind. Eng. Chem. Res. 46 (2007) 2843–2852.

[45] X.G. Hu, J.L. Pan, Y.L. Hu, Y. Huo, G.K. Li, Preparation and evaluation of solid-phase microextraction fiber based on molecularly imprinted polymers for trace

analysis of tetracyclines in complicated samples, J. Chromatogr. A 1188 (2008) 97–107.
[46] W.S. Cai, R.B. Gupta, Molecularly-imprinted polymers selective for tetracycline binding, Sep. Purif. Technol. 35 (2004) 215–222.
[47] R. Suedee, T. Srichana, T. Chuchome, U. Kongmark, Use of molecularly imprinted polymers from a mixture of tetracycline and its degradation products to produce affinity membranes for the removal of tetracycline from water, J. Chromatogr. B 811 (2004) 191.
[48] P. Wang, X.F. Fu, J. Li, J. Luo, X.Y. Zhao, M.J. Sun, Y.Z. Shang, C. Ye, Preparation of hydrophilic molecularly imprinted polymers for tetracycline antibiotics recognition, Chin. Chem. Lett. 22 (2011) 611–614.